

GENERALIZED CONTINUUM MODELS FOR GRANULAR MATERIALS: BRIDGING A TRANSITION FROM MICRO TO MACRO

Matthew R. Kuhn

Dept. of Civil and Env. Engineering, University of Portland,
5000 N. Willamette Blvd., Portland, OR, USA 97203 kuhn@up.edu

Katalin Bagi

Dept. of Structural Mechanics, Technical University of Budapest,
Budapest H-1521, Hungary kbagi@mail.bme.hu

Abstract

The paper considers possible frameworks for the transition from the micro-scale behavior of granular materials to the modeling of larger scale problems. The paper reviews direct experimental evidence that granular materials deviate from classical continuum assumptions at several length scales. Granular materials also exhibit other behaviors that are characteristic of scale-dependent materials: heterogeneity, strength that depends on specimen size, and boundary effects.

Three generalized, non-classical approaches have been used to bridge the micro-to-macro length scales: Cosserat, gradient-dependent, and non-local, integral models. One aspect of Cosserat models appears to be inconsistent with experimentally observed micro-scale behavior. The gradient-dependent approach, however, can model certain aspects of behavior when the deformation is non-uniform, and it can resolve some gross features of deformation patterning. Non-local, integral models can also be guided by experimental observations gathered from computer simulations. These experiments suggest that the integral's kernel is non-symmetric. The paper demonstrates how a simple, symmetric non-local integral model can be used to derive one of the length scales of granular materials.

Keywords: Granular material, mesomechanics, microstructure, Cosserat models, non-local models, gradient-dependent, length scale.

1. Introduction

In this paper we explore the scale-dependent behavior of dry cohesionless granular materials and its relation to some generalized continuum frameworks. Although many other materials are scale-dependent, the elemental mechanical units of granular materials are usually of microscopic size or larger, so that a number of experimental means can be applied to directly observe their micro-level behavior. More importantly, individual grains interact with each other in a relatively simple manner. With the exception of colloidal particles, long-range interactions are minimal and the interactions among grains occur primarily between pairs that are touching, with the contact forces consistent with established principles of contact mechanics. This relative simplicity allows the use of numerical, computer simulations to directly explore the micro-level and scale-dependent behavior in large assemblies of many hundreds or thousands of grains, albeit numerical grains [1]. Such simulations can capture the micro-level behavior of granular materials by modeling the individual grains in a large assembly, and they have become an important means of constructing and testing continuum descriptions of macro-level behavior. The results of some recent simulations have drawn increasing attention toward generalized, non-classical continuum descriptions of granular materials, and some of these descriptions are explored in the paper.

The outline of the paper is as follows. In Section 2, we briefly catalog many of the scale-dependent phenomena that have

been observed in granular materials and provide original experimental illustration of several such phenomena. In Section 3, we review three generalized, non-classical constitutive frameworks for incorporating microstructure into macro-level continuum descriptions of granular materials. The discussion is informed by recent experimental results that support two of the three frameworks. Section 4 explores one of the two approaches: a continuum description of non-local, integral type. Experimental results are used to calculate one of the length scales of granular materials.

2. Scale-dependent phenomena

In this section, we catalog scale-dependent phenomena that have been observed in granular materials—phenomena that are observed at one scale (or level of magnification) but are absent at other scales—although we exclude phenomena that are of large, geologic scale. The observations are from both two and three dimensional physical experiments and computer simulations.

- At the smallest meaningful scale, granular materials are composed of two elemental units: grains and the voids between them. The topological associations among these units in two dimensions can be described with a particle graph or, its dual, the void graph [2]. Dual systems can also be applied in three dimensions to model packing geometry [3], and 3D topological characteristics can be described by generalized Satake-graphs. Although a granular material may appear uniform at scales that encompass several thousands of particles, the elemental arrangement is rarely uniform or lattice-like. The graphs are highly complex and irregular, with no two particles having an identical neighborhood or micro-stiffness [4, 5]. At this micro-scale, we can think of the micro-stress as the average stress within individual particles, but this micro-stress may vary radically from one particle to another.
- At scales of a hundred or more particles, the particle displacements and rotations in 2D simulations can be quite irregular. As an example, Fig. 1 shows results from a computer simulation of 100 circular disks. The arrows show the motions of individual disks
- In 2D physical and numerical experiments with as few as a hundred grains, stress is not borne uniformly by the grains, but is instead supported by irregular, serpentine chains of particles that are roughly aligned with the major principal stress [6, 7]. The intensity of stress is, therefore, highly localized within a granular material, and the concept of an average meso-stress may only have meaning at length scales of, perhaps, several or more particle diameters. Some statistical measures have been developed for describing the distribution of the disparate contact forces among particles [8, 9], but their spatial distribution has not yet been adequately addressed.
- At scales that encompass many hundreds or a few thousands of 2D particles, a number of localized deformation structures become prevalent: vortex-like circulation cells [10], microbands of shearing deforming [11], and dilation clusters. An example of dilation clustering is shown in Fig. 2, which presents the micro-level distribution of dilation rates within a dense two-dimensional assembly of 4008 irregularly packed circular disks. In this computer simulation, the entire assembly was deformed in simple shear un-

while the assembly was being compressed vertically and expanded horizontally. The figure reveals several groups of particles, with the particles in each group moving in conformance as micro-scale clusters.



Figure 1: *Clustering within an assembly of 100 granules*

der constant vertical stress. Only positive volume changes (dilation) can be represented in this monochrome plot, but even while the entire material is intensely dilatant, about 38% of its volume is compressing. The dilation is concentrated within numerous clusters, each containing a few tens of particles.

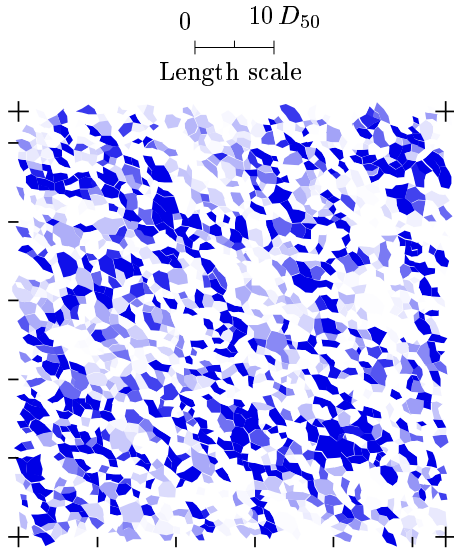


Figure 2: *Dilation clustering in an assembly of 4008 granules*

- Shear bands are observed within assemblies of several thousand or more particles in 2D experiments. When viewed at a larger scale, these bands may appear as discontinuity surfaces, but in carefully observed physical and numerical experiments on 2D and 3D materials, shear bands have measurable thicknesses of between 8 and 20 particle diameters [12, 13]. Within the bands, meso-sized clusters of particles can rotate in circulation patterns in either clockwise or counter-clockwise motions (Fig. 3), although the dominant direction of cluster rotation is consistent with the direction of shear. Once formed, shear bands are stationary and persistent on a macro-scale, although micro-scale studies reveal that shear bands may locally shift and change in thickness over time [14].

Besides these examples of the scale-dependent patterning of stress and deformation, granular materials also exhibit certain

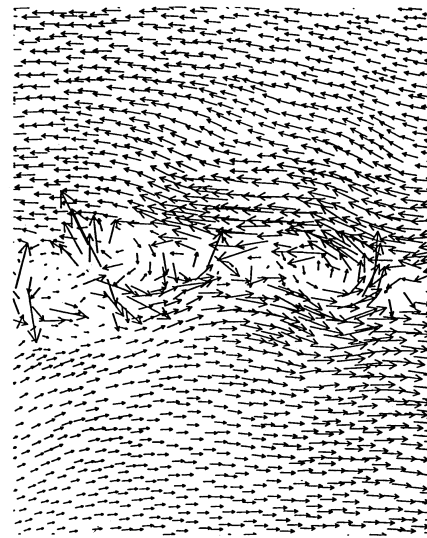


Figure 3: *Particle velocities in a 2D assembly of disks. Circulation patterns are visible within a shear band*

behaviors that are associated with scale dependence:

- Strength heterogeneity: The heterogeneity of granular materials is one of their distinguishing characteristics, and material non-uniformity is present at every scale. Bagi et al. [15] found that the randomness of micro-geometry in granular rocks leads to a significant scatter in fracture strength. The variation of strength in cohesionless granular materials is illustrated in Fig. 4, which shows the results of simulated shear tests on 2D samples of 1002 densely packed circular disks. One hundred assemblies were com-

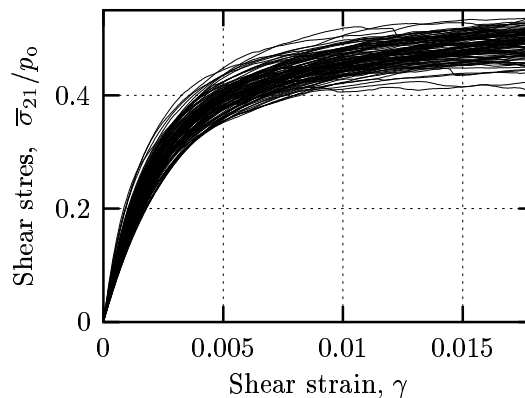


Figure 4: *Variation in the shearing behavior of 100 specimens of 2D assemblies of disks.*

packed from initially sparse arrangements of the same particle set, so

that the compacted assemblies had the same solids fraction and the same particle sizes. Figure 4 shows considerable scatter in strength even under these ideal conditions. At small scales, as in the assembly represented in Fig. 1, strength variations are, of course, the natural consequence of an irregular particle topology (micro-fabric). At larger scales, variations can result from differences in the material macro-fabric, as measured by void ratio or by distributions in particle size or contact orientations.

- **Size effect on strength:** Bažant [16] has presented a review of the effects of specimen size upon strength, showing that for most materials—metallic, ceramic, and cemented—strength increases with diminishing specimen size. An opposite trend might occur in granular materials. Using methods identical to those described in the previous paragraph, two sets of granular assemblies were constructed: one set with 200 circular disks per assembly, the other set with 1002 disks per assembly. The two sets had nearly the same macro-fabric, as was evident in the distributions of particle sizes, initial mean stresses, void ratios, and coordination numbers. Although the scatter in strengths was greater in the smaller assemblies, the strength was, on average, smaller than in the larger assemblies. The mobilized friction angle was about 25.44° for the assemblies of 200 particles and about 25.94° in the 1002-particle assemblies (results from the latter set were shown in Fig. 4). Although the differences were slight, the different coordination numbers and mean stresses of the two sets may have produced the different strengths, and further investigation is required.
- **Boundary effects:** Edelen [17] demonstrated how boundary effects, and in particular the surface tension at fluid interfaces, can result from the non-local nature of particle (i.e. molecular) interactions. A solid grain only interacts directly with the neighboring grains that it touches, but different phenomena can be observed near the boundaries of granular assemblies. Onda [18] has shown, for example, that the micro-mechanisms that trigger granular avalanching at a free surface

are different from the mechanisms that predominate within a granular material's interior. At a rigid platen surface, particle motions are also influenced in a manner that is not present further from the surface.

3. Generalized continuum frameworks

We briefly consider three generalized, non-classical continuum models: Cosserat models, gradient-dependent models, and non-local, integral-type models. Each of these constitutive models introduce materials properties with dimensional units other than those of stress, so that a characteristic length is embedded within their descriptions. This length can serve as a bridge between behaviors at different scales. As an example, Cosserat descriptions have been proposed for granular materials and have been incorporated into finite element models [19, 20]. When viewed at a scale of several thousand times the characteristic length, a shear band appears as a displacement discontinuity, but when considered at a second, smaller scale, these Cosserat models can resolve deformation contours within a band. A continuum model will, however, require more than a single characteristic length to resolve phenomena that occur at more than two scales (for example, to resolve the even finer detail of microband patterning).

Although Cosserat models can be calibrated to reproduce the observed characteristics of shear bands, there are reasons to suspect whether they truly capture the micro-behavior of granular materials at scales of several particle diameters. In the Cosserat framework, rotations and displacements are treated as independent fields, so that the rotation of a material point, perhaps a single grain or cluster, can differ from the mean rotation of its neighborhood (the skew symmetric part of the macro-scale velocity gradient). Recent experiments have shown, however, that the mean particle rotation is very nearly equal to the mean rotation of the particle neighborhood. This evidence comes from studies of 2D assemblies in which the macro-level deformation was either spatially uniform [21] or spatially nonuniform [14]. Other evidence has shown that particle rotations are highly variable, and in 2D studies, the direction of rotation can alternate from clockwise to counter-clockwise as observation moves from one neighboring particle to another, or from one cluster to another. Within a

shear band, the rotation direction of a single particle can also change with time, even when the loading is proportional and monotonic [22]. It may be difficult, therefore, to resolve such strong micro-level fluctuations as the projection of a continuum field onto a micro-neighborhood, even a field that intentionally models micro-rotations. Further investigation of this matter is certainly required.

In a recent experimental study, the shearing behavior of granular materials was found to depend on the first and second gradients of shearing strain [14]. This dependence is subtle and was only resolved by averaging the behaviors of numerous material meso-samples that were subjected to the same non-uniform deformation field. The dependence of shearing stress on the *first* strain gradient was altogether absent at small strains, but the effect of the first gradient became quite strong during the subsequent plastic deformation. The effect of the *second* strain gradient was present at both small and large strains, although its effect at small strains was opposite that at larger strains. The separate influence of the two strain gradients suggests that at least two different characteristic lengths can be included in a gradient-dependent continuum description, so that material behavior can be resolved at three scales: macro, meso, and micro. The study showed that the measured effects of the two strain gradients were consistent with certain features of both shear band and microband deformation structures—localized deformation patterns that are apparent at two different scales. We should note that the gradient dependence was measured by averaging multiple meso-sized samples without regard to variations among the samples. These micro-fluctuations are the likely cause of spatial irregularities in the patterning of force chains, microband deformations, and shear bands.

A number of explicitly non-local, integral-type models have been proposed as a means of including a characteristic length within a continuum description of material behavior [23, 24, 25]. In this approach, the stress at a material point \mathbf{x} or its neighborhood is expressed as a functional of the strain in a finite neighborhood \mathcal{B} , usually as an averaged strain $\bar{\boldsymbol{\varepsilon}}$. The strain $\boldsymbol{\varepsilon}$ in the surrounding region \mathcal{B} is averaged with a weighting kernel Φ :

$$\bar{\boldsymbol{\varepsilon}}(\mathbf{x}) = \int_{\mathcal{B}} \Phi(\mathbf{x} - \mathbf{x}') \boldsymbol{\varepsilon}(\mathbf{x}') dV, \quad (1)$$

where the kernel Φ is either a scalar or a fourth order tensor. If the kernel Φ is restricted to the scalar Dirac operator δ , then the strain $\bar{\boldsymbol{\varepsilon}}$ is simply the local strain $\boldsymbol{\varepsilon}$. In the usual approach, however, the kernel Φ is assumed to be smooth and centrally symmetric, such that $\Phi(\mathbf{a}) = \Phi(-\mathbf{a})$. A centrally symmetric kernel can take the form of a scalar function $\phi(|\mathbf{x} - \mathbf{x}'|)$, where the argument is an appropriate norm of the vector $\mathbf{x} - \mathbf{x}'$ (e. g., the objective Euclidean norm). With this restriction, the strain $\bar{\boldsymbol{\varepsilon}}$ can be expanded as a series in $\boldsymbol{\varepsilon}$ and its *even*-order derivatives, showing that second gradient models are but special instances of this restricted integral form [26, 25]. The restriction excludes the possible effect of the first and other odd-order strain gradients on the material behavior. The experimentally measured effect of the first strain gradient in granular materials suggests, however, that the condition of central symmetry on Φ is unduly restrictive.

We briefly consider a kernel composed of symmetric and anti-symmetric parts, with $\Phi = \Phi^{\text{sym}} + \Phi^{\text{anti}}$, as a means of capturing the effects of both even and odd ordered strain gradients. The anti-symmetric part Φ^{anti} introduces certain difficulties, notably that its integration over a symmetric, spherical region \mathcal{B} is identically zero. If region \mathcal{B} is allowed to be non-spherical, then we can do one of the following: 1) assign a preferred orientation to \mathcal{B} to capture anisotropy in that direction, or 2) apply Φ^{anti} to an objective and scalar function of the strain $\boldsymbol{\varepsilon}(\mathbf{x}')$. As an example of the latter, we could multiply an anti-symmetric Φ by a function of the strain invariants. Marcher and Vermeer [27] present a non-local elasto-plastic model in which the volumetric strain rate is averaged with a *symmetric* kernel,

$$\int_{\mathcal{B}} \phi^{\text{sym}}(|\mathbf{x} - \mathbf{x}'|) \dot{\varepsilon}_v^p(x') dV, \quad (2)$$

where the scalar valued ϕ^{sym} is a symmetric error function, as will be detailed further below. This approach can be extended to non-symmetric forms, such as the following:

$$\frac{1}{2} \int_{\mathcal{B}_{1/2}} \left\{ \begin{aligned} &\phi^{\text{sym}}(|\mathbf{x} - \mathbf{x}'|) \\ &[\dot{\varepsilon}_v^p(\mathbf{x}') + \dot{\varepsilon}_v^p(-\mathbf{x}')] \\ &+ \phi^{\text{anti}}(|\mathbf{x} - \mathbf{x}'|) \\ &|\dot{\varepsilon}_v^p(\mathbf{x}') - \dot{\varepsilon}_v^p(-\mathbf{x}')| \end{aligned} \right\} dV \quad (3)$$

which contains the symmetric (even)

and anti-symmetric (odd) scalar valued functions ϕ^{sym} and ϕ^{anti} . The region $\mathcal{B}_{1/2}$ is a hemispherical region, but because we integrate the absolute value of the anti-symmetric part, the orientation of $\mathcal{B}_{1/2}$ is of no consequence. Only the integrated magnitude of the anti-symmetric spatial variations in ε_v^p are included, so that an equal gradient of ε_v^p in any direction will have an equal effect on the non-local response. Integrals of the form (3) could also be applied to other strain invariants or to functions of several invariants.

4. A characteristic length

We will now consider only the symmetric part of Eq. (3) and compute one of the characteristic lengths for granular materials. The calculation will be based upon the experimental results of Kuhn [14], who measured the effect of the second strain gradient on the low-strain shear modulus G in a 2D assembly of circular disks. The modulus was found to depend upon the second derivative of the shear strain γ in the following manner:

$$G = G_o + B_2 \frac{\gamma''}{\gamma}, \quad (4)$$

where the moduli G_o and B_2 were experimentally measured. In the experiments, the shear strain γ varied in a single coordinate direction x_2 , and the differentiation γ'' in Eq. (4) is taken in that direction. We will consider a 2D material region within which the shear strain varies in a quadratic manner,

$$\gamma = \gamma_o + \frac{1}{2} \gamma_o'' x_2^2, \quad (5)$$

and then use Eq. (1) to find an averaged strain $\bar{\gamma}$ within the region. To be consistent with the experimental measurements, the product of the non-local $\bar{\gamma}$ and the base modulus G_o should equal the product of the local γ_o and the corrected modulus G in Eq. (4), or

$$\bar{\gamma} = \gamma_o + \frac{B_2}{G_o} \gamma_o''. \quad (6)$$

As the choice of an averaging kernel, we return to the symmetric form suggested by Marcher and Vermeer [27] as a symmetric version of Eq. (3):

$$\bar{\gamma} = \frac{1}{A} \int_{\mathcal{B}} \frac{1}{\ell \sqrt{\pi}} \gamma(x'_2) e^{-(|\mathbf{x}-\mathbf{x}'|/\ell)^2} dV. \quad (7)$$

In this form, ℓ is the characteristic length that we will calculate and A is the value of the integral when $\gamma = 1$ ($A = \ell \sqrt{\pi}$ for a circular two dimensional region of infinite extent).

Substituting Eq. (5) into Eq. (7) gives the following value of $\bar{\gamma}$:

$$\bar{\gamma} = \gamma_o + \ell^2 \gamma_o'' / 4. \quad (8)$$

Comparing Eqs. (8) and (6) we see that ℓ is directly related to the experimentally measured values of B_2 and G_o :

$$\ell = 2 \sqrt{B_2 / G_o}. \quad (9)$$

For experiments on 2D assemblies, the ratio B_2/G_o was found to range from 0.55 to $0.87 D_{50}^2$, where D_{50} is the mean particle diameter. These values yield a length scale ℓ of between $1.5 D_{50}$ and $1.9 D_{50}$. With the particular error function in Eq. (7), about 63% of the stress at a material point is attributed to the deformation within a circular region of radius ℓ centered at the point. The small computed values of ℓ suggest that the measured dependence of shear stress upon the second strain gradient at low strains will only affect the material behavior at small distances. This result is consistent with the work of Chang and Gao [28] who derived similar values of the ratio B_2/G_o from the mechanics of a simple two-particle system. Even at such distances, however, the particular length scale ℓ may be associated, however, with the microband deformation patterning that occurs at very low strain, since microbands have a spatial periodicity of only $3.5 D_{50}$ to $8 D_{50}$.

References

- [1] Cundall, P.A., Strack, O.D.L. (1979), *Géotechnique*, **29**, No. 1, pp. 47.
- [2] Satake, M. (1992), *Int. J. Engng. Sci.*, **30**, No. 10, pp. 1525.
- [3] Bagi, K. (1996), *Acta Technica Acad. Sci. Hung.*, **107**, pp. 1.
- [4] Tsuchikura, T., Satake, M. (2001), In: *Powders and Grains 2001*, Kishino, Y., (Ed), A.A. Balkema, Lisse, pp. 29.
- [5] Yang, R.Y., Zou, R.P., Yu, A.B. (2001), In: *Powders and Grains 2001*, Kishino, Y., (Ed), A.A. Balkema, Lisse, pp. 11.

- [6] Drescher, A., de Josselin de Jong, G. (1972), *J. Mech. Phys. Solids*, **20**, pp. 337.
- [7] Cundall, P.A., Drescher, A., Strack, O.D.L. (1982), In: *Deformation and Failure of Granular Materials*, Vermeer, P., Luger, H., (Eds), A.A. Balkema, Rotterdam, the Netherlands, pp. 355.
- [8] Coppersmith, S., Liu, C.h., Majumdar, S., Narayan, O., Witten, T. (1996), *Physical Review E*, **53**, No. 5-A pt A, pp. 4673.
- [9] Mueth, D.M., Jaeger, H.M., Nagel, S.R. (1998), *Physical Review E*, **57**, No. 3-B, pp. 3164.
- [10] Williams, J.R., Nabha, R. (1997), *Mech. of Cohesive-Frictional Mat.*, **2**, No. 3, pp. 223.
- [11] Kuhn, M.R. (1999), *Mech. of Materials*, **31**, No. 6, pp. 407.
- [12] Bardet, J.P., Proubet, J. (1991), *Géotechnique*, **41**, No. 4, pp. 599.
- [13] Vardoulakis, I. (1998), In: *Behaviour of Granular Materials*, Cambou, B., (Ed), Springer, Vienna, pp. 339.
- [14] Kuhn, M.R. (2002), *J. Mech. Phys. Solids*, in review.
- [15] Bagi, K. (2001), *Rock Mechanics*, in review.
- [16] Bažant, Z.P. (1999), *Arch. Appl. Mech.*, **69**, No. 9–10, pp. 703.
- [17] Edelen, D.G.B. (1976), In: *Continuum Physics, Vol. IV—Polar and Nonlocal Field Theories*, Eringen, A.C., (Ed), Academic Press, New York, pp. 76.
- [18] Onda, Y., Matsukura, Y. (1997), *Earth Surface Processes and Landforms*, **22**, No. 4, pp. 401.
- [19] Mühlhaus, H.B., Vardoulakis, I. (1987), *Géotechnique*, **37**, No. 2, pp. 271.
- [20] de Borst, R. (1991), *Engineering Computations*, **8**, No. 4, pp. 317.
- [21] Calvetti, F., Combe, G., Lanier, J. (1997), *Mech. of Cohesive-Frictional Mat.*, **2**, No. 2, pp. 121.
- [22] Boulon, M., Hassan, A.N. (1998), In: *Localization and Bifurcation Theory for Soils and Rocks*, Adachi, T., Oka, F., Yashima, A., (Eds), A.A. Balkema, Rotterdam, pp. 59.
- [23] Kröner, E. (1967), *Int. J. Solids and Structures*, **3**, pp. 731.
- [24] Bažant, Z.P., Belytchko, T.B., Chang, T.P. (1984), *J. Engrg. Mech.*, **110**, No. 12, pp. 1666.
- [25] Vardoulakis, I., Aifantis, D.C. (1991), *Acta Mechanica*, **87**, No. 3, pp. 197.
- [26] Koenders, M.A. (1990), *J. Energy Res. Tech.*, **112**, No. 1, pp. 51.
- [27] Marcher, T., Vermeer, P.A. (2001), In: *Continuous and Discontinuous Modelling of Cohesive-Frictional Materials*, Vermeer, P.A., Diebels, S., Ehlers, W., Herrmann, H.J., Luding, S., Ramm, E., (Eds), Springer, Berlin, pp. 89.
- [28] Chang, C.S., Gao, J. (1995), *Int. J. Solids and Structures*, **32**, No. 16, pp. 2279.